

Optimising Power Allocation in LoRaWAN IoT Applications

Yousef A. Al-Gumaei, Nauman Aslam, Xiaomin Chen, Mohsin Raza, Rafay Iqbal Ansari

Abstract—Long Range Wide Area Network (LoRaWAN) is one of the most promising IoT technologies that are widely adopted in low-power wide-area networks (LPWAN). LoRaWAN faces scalability issues due to a large number of nodes connected to the same gateway and sharing the same channel. Therefore, LoRa networks seek to achieve two main objectives: successful delivery rate and efficient energy consumption. This paper proposes a novel game theoretic framework for LoRaWAN named Best Equal LoRa (BE-LoRa), to jointly optimize the packet delivery ratio and the energy efficiency (bit/Joule). The utility function of LoRa node is defined as the ratio of the throughput to the transmit power. LoRa nodes act as rational users (players) which seek to maximize their utility. The aim of the BE-LoRa algorithm is to maximize the utility of LoRa nodes while maintaining the same signal-to-interference-and-noise-ratio (SINR) for each SF. The power allocation algorithm is implemented at the network server, which leads to an optimum SINR, spreading factors (SFs) and transmission power settings of all nodes. Numerical and simulation results show that the proposed BE-LoRa power allocation algorithm has a significant improvement in packet delivery ratio and energy efficiency as compared to the Adaptive Data Rate (ADR) algorithm of legacy LoRaWAN. For instance, in very dense networks (624 nodes), BE-LoRa can improve the delivery ratio by 17.44% and reduce power consumed by 46% compared with LoRaWAN ADR.

Index Terms—Internet of Things, LoRaWAN, Game Theory, Power Allocation, SINR balancing.

I. INTRODUCTION

MANY emerging Internet-of-Things (IoT) applications require low cost, long range and energy efficient wireless communication frameworks to share the data. Some examples of these applications are agriculture, smart home, energy engagement, smart metering, healthcare, industries, and smart cities. The proprietary technologies of Low power wide area network (LPWAN) such as Sigfox [1], Narrow-Band NB-IoT [2], Weightless [3], and LoRaWAN [4] have gained much interest in last few years. LPWAN is a promising technology which allows a large number of small end devices (nodes) to connect to one or more wireless gateways. LPWAN is a suitable solution for such applications as other wireless technologies (Bluetooth, WiFi, and ZigBee) are not able to provide long range communication. On the other hand, use of cellular networks for machine-to-machine (M2M) communication is expensive and consumes a lot of power [5].

Y. A. Al-Gumaei, N. Aslam, X. Chen, R. I. Ansari are with Department of Computer and Information Science, Northumbria University, UK (email: dr.alguamei@gmail.com, nauman.aslam@northumbria.ac.uk, xiaomin.chen@northumbria.ac.uk, rafay.ansari@northumbria.ac.uk).

M. Raza is with Department of Computer Science, Edge Hill University, UK (Email: mohsinraza119@gmail.com).

The Long Range (LoRa) patented by (Semtech) uses chirp spread spectrum (CSS) modulation techniques in which the chirps are used to transmit the data [6]. In LoRaWAN, thousands of end devices can connect to the internet servers via a single gateway [7]. LoRaWAN builds on the top of LoRa physical layer which enables it to consume low power and communicate over distances of several kilometers [8]. The Spreading Factors (SFs) are assumed to be completely orthogonal to each other for interference free communications. However, a large number of nodes, simultaneous transmission of nodes having the same SF, and interference due to other co-located networks operating on the same unlicensed frequency bands is still a challenge for LoRaWAN scalability. One solution to address such challenges is to adapt the LoRa operating parameters such as SF and transmission power. In LoRaWAN, the Adaptive Data Rate (ADR) algorithm adapted these parameters to improve the communication performance of LoRa networks, but it has not investigated the impact of the number of LoRa nodes in the network. Moreover, the ADR algorithm used the maximum signal-to-noise-ratio (SNR) of the last 20 records to update the SF and power settings of nodes, but it is not the optimal and may cause higher power consumption by the nodes.

Therefore, this paper aims to design an efficient power allocation algorithm to reduce nodes' transmit powers to the level that ensures successful transmission, mitigates interference and improves system's energy efficiency. Game theory is one of the techniques that has been used to implement power allocation algorithms. In a power allocation algorithm, the number of nodes in each SF depends on the processing gains and the threshold SNR, while the update of transmission power depends on the optimal value of signal-to-interference-and-noise ratio (SINR). Our proposed solution significantly increases both the packet delivery ratio and the energy efficiency of communications over the ideal channel.

A. Related work and motivation

LoRaWAN has been deployed in different countries, but the scalability of these networks is still a matter of active research due to a number of challenges [9]. Among these challenges, energy efficiency and interference are the most significant as they affect packet delivery. Assuming complete orthogonality among SFs, the co-SF interference caused by transmissions over the same channel has the highest impact on packet delivery when the SINR of the desired transmission is below the required threshold. Thus, the performance of the nodes that are located farthest from the gateway is reduced

greatly due to the "capture effect" [10], which occurs when a weaker signal is suppressed by a much stronger signal transmitted by the nodes located closer to the gateway [11].

To the best of our knowledge, limited research has been conducted on addressing the scalability of LoRaWAN based on the packet collision, interference, and power allocation. The problems of scalability and the LoRa performance have been analyzed using simulations in [12], [13], and [14] without considering ADR or any other SF and power allocation adaptation algorithms. The evaluation of the link level performance of LoRa has been presented in [15], in which the numerical results show that the collisions between packets with different SFs can cause packet loss due to high interference. In [9], the performance of a LoRa system was analyzed under the capture effect, in which the signal-to-interference-ratio (SIR) of a desired signal should be above the required threshold for successful packet reception. The co-SF interference was modeled using stochastic geometry. Authors in [16] evaluated the scalability and throughput of LoRaWAN deployments based on the capture effect and coverage models under the impact of co-SF and inter-SF interference. Therefore, the system level performance of a LoRa network based on the interaction behavior between the self-interested LoRa nodes in the same SF is yet to be modeled and investigated. In [17], allocating resources amongst the available servers has been studied using a combination of LoRaWAN and traditional public safety networks and a self enforcing agreement was established based on game theory. This combination and the self enforcing agreement were not used to optimize the transmission resources between nodes and gateway. In the subsequent, we present the contributions and unique aspects of this work.

B. Contributions

In this paper, it is demonstrated that by using optimal power control, LoRaWAN nodes can maximize packets delivery ratio, reduce collisions and improve energy efficiency. This paper proposes SINR balancing using optimal power allocation such that all packets received at the gateway have the same signal power. Nodes located at a shorter distance from the gateway can achieve SINR balancing by using lower transmission power resulting in the significant reduction of their own energy as well as the overall energy of the system. To achieve this balancing, a best equal SINR power allocation (BE-LoRa) to improve the performance of LoRaWAN is proposed. The problem of power allocation is formulated as a non-cooperative power control game to define the utility function and game model. The non-cooperative power control model is used to derive the proposed BE-LoRa scheme by assuming equal SINR of received packets at the gateway. The process involves computation of optimal SINR values at the network server which are used to allocate SFs, update the power settings and send these new settings to LoRa nodes as ADR commands. The computation of optimal SINR is performed by considering key network parameters such as the number of active LoRaWAN nodes and their processing gains. In this work, class A LoRa nodes are able to increase

SF if the uplink transmission cannot reach the gateway. If there is no downlink frame received by a LoRa node, the node increases the SF for the following uplink frame. This increases the probability of reaching a gateway and receiving the new settings acknowledgment (ACK) of SF and transmission powers from the network server via the two short downlink windows. The network server assists the nodes by sending the final settings of SF and transmission power via two short downlink windows and this cooperation leads to performance optimization at LoRa nodes. The network server starts to assign SFs to the nodes based on the received RSSI and the total number of nodes in the system. The number of nodes in each SF is based on the percentage that has been computed at the target SINR and guarantees that all nodes can maintain this target. Next, the network server computes the best equal SINR (optimal SINR) based on the number of nodes in each SF and updates the nodes' transmission power levels based on these optimal values. Based on the channel condition of the node, the network server is able to update (decrease or increase) node's transmission power to achieve this optimal SINR until all nodes reach equilibrium. At equilibrium, all nodes achieve the same optimal SINR, though different power transmission levels are used. Furthermore, the energy consumption of a particular node is the total energy used by the node divided by the number of messages received by the network server. Reducing the power level of nodes with good channel conditions not only leads to decreased interference but also improves the energy efficiency of the system. The key contributions of this paper are summarized as follows:

- 1) *Design*: A best equal SINR (BE-LoRa) power allocation algorithm is designed to improve the energy efficiency performance and the packet delivery ratio of LoRaWAN.
- 2) *Implementation*: BE-LoRa power allocation is implemented using a game theoretic framework. A suitable utility function is proposed, which satisfies the trade-off between the probability of packet success rate and the power consumption. For the sake of demonstration, the BE-LoRa power allocation is implemented in a single cell scenario, however, it is also applicable to a multi-cell scenario.
- 3) *Analysis and Comparison*: In addition, the BE-LoRa algorithm is formulated analytically and a simulation model is presented. The results have been compared with the legacy LoRaWAN ADR.

The remainder of this paper is organized as follows. Section II provides a background on the LoRaWAN networks, architecture, and type of classes used in communications. Section III describes the system model of LoRaWAN. Section IV presents the non-cooperative power allocation approach that results in Nash equilibrium solution. Section V presents the BE-LoRa scheme. Section VI presents the numerical results of the proposed scheme and a comparison with the legacy LoRaWAN ADR. Finally, Section VII concludes this paper and discusses future directions of this work.

TABLE I
LoRaWAN CONFIGURATION TABLE [19]

Configuration	Bit rate [b/s]	Required SNR [dB]
SF12 / 125 kHz	293	-20.0
SF11/ 125 kHz	537	-17.5
SF10 / 125 kHz	976	-15.0
SF9 / 125 kHz	1757	-12.5
SF8 / 125 kHz	3125	-10.0
SF7 / 125 kHz	5469	-7.5

II. LoRaWAN BACKGROUND

A. LoRaWAN overview

LoRaWAN is developed as an open standard by LoRa Alliance [4]. LoRa itself refers to long range and is a physical layer modulation technique derived from chirp spread spectrum (CSS) technology. LoRa is proprietary standard owned by Semtech and patented in 2014 [18]. LoRa implements CSS modulation to improve receiver sensitivity, noise immunity and interference avoidance. The LoRaWAN architecture uses star topology in which the end devices (nodes) transmit and received signals at a single or multiple access points (gateways). These gateways forward the received packets to the network servers which are connected over the standard Internet protocol (IP) network. In addition, network servers are also connected to the application servers over IP.

In LoRaWAN, the theoretical bit rate at SF k , $k = 7, 8, 9, \dots, 12$, is given by:

$$R^{\text{SF}_k} = \frac{BW \times \text{SF}_k \times CR}{2^{\text{SF}_k}} \quad (1)$$

where BW is the bandwidth in [Hz], CR is the code rate and SF indicates spreading factor.

Table I summarizes the bit rate and SNR at $BW=125$ kHz for the LoRaWAN configuration considered in this paper.

B. LoRaWAN communication

The nodes in LoRaWAN can be implemented in three different classes:

- 1) Class A: LoRaWAN devices in this class have lowest power consumption. Nodes in Class A use pure ALOHA, and it opens two receive windows at specific times after an uplink transmission. The network server can respond by sending the acknowledgement (ACK) to one of these windows but not both. In case of receiving ACK in the first window, the node will not open the second receive window and if the network server does not respond in either of these windows, the node retransmits the message until ACK is received.
- 2) Class B: it is extendable to class A in which the nodes are synchronized using periodic beacons sent by the gateway to allow the scheduling of additional receive windows for ACK messages. The time between two scheduling receive windows is known as ping period and the time between two beacons (including the two received windows of class A) is known as the beacon period [20]. The power consumption in this class depends on the downlink traffic.

- 3) Class C: nodes using this class keep the receiving time slot open except when they are in transmission mode. The power consumption of this class is the highest due to the higher channel listening times.

Typically, class A and B nodes are battery-powered, while class C devices are powered by the electrical network due to the higher energy requirements [21].

In LoRaWAN, nodes can adapt data rate if uplink transmissions are not followed by a downlink response from the network. A node begins to step up transmit power level to the maximum before doing the same for spreading factor to improve the robustness of the link [22]. Increasing transmit power can establish more reliable communications but it compromises energy efficiency. Moreover, a node can also request the network server to monitor and control the communication link between itself and the gateway by setting the ADR bit to be 1 (ADR =1) in the uplink message. When the network server detects the ADR bit as 1, it compares the link quality of the last e.g. 20 packets received with the margin SNR. If the link quality is higher than the margin SNR, the network decides to reduce SF and then the transmit power of that particular node. This reduction will decrease the data rate and reduce power consumption. It is found that the ADR decision of updating SF or transmission power for a particular node is dependent on the channel conditions, without considering the impact of the interference resulting from the increasing number of nodes.

III. SYSTEM MODEL

In this paper, wireless LoRaWAN network with M class A LoRaWAN nodes is considered, which are distributed around one base station (gateway) located at the cell centre. It is assumed that all LoRaWAN nodes inside the cell can successfully communicate with the gateway using the available sets of spreading factors and transmit powers. In this work, nodes do not update the spreading factor when the channel conditions change as in the ADR scheme, but the SF_k are assigned to the nodes by network server based on the received RSSI and the percentage number of nodes in each SF. The subscript k has a range of $k = 7, 8, \dots, 12$. As shown in Fig. 1, SF is assigned to nodes based on RSSI and the interference occurs when the same SF nodes are transmitting simultaneously.

The path loss model between the nodes and the gateway is considered to be the log-distance path model with shadowing [23]. The received power $p_{\text{rec},i}$ of packet send by node i is given by

$$p_{\text{rec},i}[\text{dB}] = p_i - PL(d_0) - 10n \log_{10} \left(\frac{d_i}{d_0} \right) + X_\sigma \quad (2)$$

where p_i is transmit power of node i , $PL(d_0)$ is the mean path loss at the reference distance d_0 in [dB], d_i is the distance between node i and the gateway, n is the path loss exponent, and X_σ is a zero-mean Gaussian distributed random variable with standard deviation σ [dB]. The path loss model is highly dependent on the environment. Based on the empirical measurements in [12], given $d_0 = 40\text{m}$, it is determined that in the considered environment $PL(d_0)$ is 127.41dB, n is 2.08

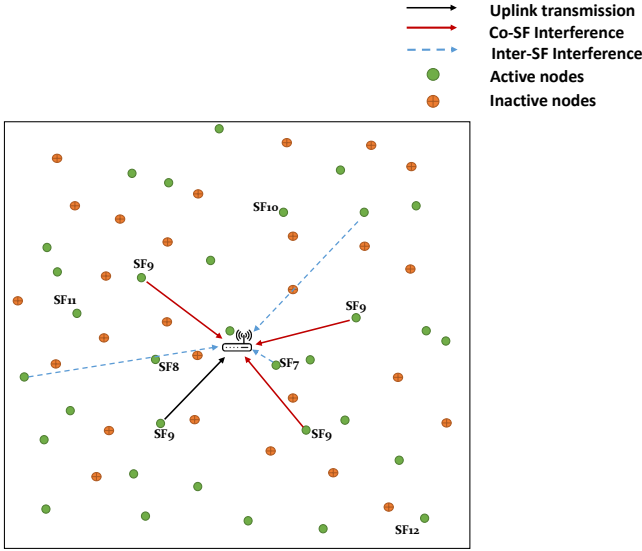


Fig. 1. System model of LoRaWAN

and σ is 3.57 dB. To investigate the performance of a single LoRaWAN node under the simultaneous interfering transmissions, only co-SF interference is considered. The impact of inter-SF interference is negligible due to the orthogonality of SFs and the lower value of the margin SIR between different SFs.

The processing gain $G_p^{\text{SF}_k}$ for SF k can be calculated by [24]:

$$G^{\text{SF}_k} = 10 \cdot \log_{10} \left(\frac{R_c}{R_b^{\text{SF}_k}} \right) \text{ dB} \quad (3)$$

where $R_c = BW$ is the chip rate (chips/second) and $R_b^{\text{SF}_k}$ is the bit rate (bits/second) as presented in Eq. (1). The processing gain in each SF is a value in dB which is added to the received signal to ensure that signals can be decoded successfully. It increases by 2.5dB between two consecutive SFs.

The signals sent by nodes with the same or different SFs can overlap in time and frequency at the receiver. In such cases with simultaneous reception of packets, the demodulator output can be indistinct depending on the signal to interference ratio threshold (i.e. $\text{SIR} \approx \text{SINR}$) [16]. Any signal with SF_k can be decoded correctly only if the SIR of the received signal compared to interference signals (interference plus noise) is above the margin. The SIR margin for two cases, inter-SF interference (different SF) and co-SF interference (same SF) are presented in Table II., [25]:

Table II highlights that the highest SIR margins occur when the desired and interfering signals have the same SF. Thus, we can conclude that any packet can be received and decoded successfully if the SIR is greater than the highest margin SIR (6 dB) regardless of the spreading factor, SF. The SINR of node i with a spreading factor SF_k has the following general form [14]:

$$\gamma_i^{\text{SF}_k} = \frac{G_i^{\text{SF}_k} p_{\text{rec},i}}{\sigma^2 + \sum_{j=1, j \neq i}^{M_k} p_{\text{rec},j}} \quad (4)$$

TABLE II
SIR MARGIN BETWEEN THE DESIRED SIGNAL AND THE INTERFERING SIGNAL [25]

SIR [dB]	7	8	9	10	11	12
7	6	-16	-18	-19	-19	-20
8	-24	6	-20	-22	-22	-22
9	-27	-27	6	-23	-25	-25
10	-30	-30	-30	6	-26	-28
11	-33	-33	-33	-33	6	-29
12	-36	-36	-36	-36	-36	6

where $G_i^{\text{SF}_k}$ is the processing gain of the i th LoRa node, $p_{\text{rec},i}$ is the received power of node i , $p_{\text{rec},j}$ is the received power of the interfering node j which uses the same SF, and σ^2 is the additive white Gaussian noise.

It is noted that SINR of node i is highly affected by interfering transmissions from the same SF (i.e. co-SF), compared to the interference caused by signals using different SFs (inter-SF). Thus, the summation of powers in the denominator of Eq. (4) represents the co-SF interference. To ensure successful decoding of a packet received from node i , the following inequality holds:

$$\gamma_i^{\text{SF}_k} \geq \Gamma_i \quad (5)$$

where Γ_i is the target SINR.

IV. NON-COOPERATIVE POWER ALLOCATION GAME

A. LoRa node utility function

LoRaWAN gateway uses the cyclic redundancy check (CRC) to detect errors at the receiver such that the probability of undetected transmission errors is negligible. When the gateway detects an error in a packet, it will request a packet re-transmission. With perfect error detection, we can express the packet success rate (PSR) as $P_s = (1 - P_b)^L$, where P_b is the bit error rate and L is the length of packet in bits. To achieve successful packet delivery with minimal power consumption, we need to express the utility function as a ratio of throughput to transmit power. In a game model, all nodes will seek to maximize this utility by selecting their transmit power from the power strategy set. In case of transmit power $p_i = 0$, for all modulation schemes, the best strategy for the receiver is to make a guess for each bit, resulting in $P_s = 2^{-L}$, resulting in infinite utility [26]. To avoid the utility maximization solution to be $p_i = 0$, we approximate the PSR using an efficiency function that closely follows the behavior of PSR, while producing $P_s = 0$ when the transmit power equals to 0. The efficiency function should closely follow the PSR of a specific modulation. In [26], authors investigated the PSR for various modulation schemes. In this work, the popular approximation of PSR for the CSS modulation is used:

$$f_i(\gamma_i^{\text{SF}_k}) = (1 - 0.5e^{-\alpha \gamma_i^{\text{SF}_k}})^L \quad (6)$$

where $f_i(\gamma_i^{\text{SF}_k})$ refers to the efficiency function, and α is a constant which depends on the system modulation. The efficiency function is a sigmoid function which has the following properties:

- 1) $f : [0, \infty] \rightarrow [0, 1]$ is continuous,
- 2) $f(0) = 0$ and $\lim_{(\gamma^{\text{SF}_k}) \rightarrow \infty} = 1$

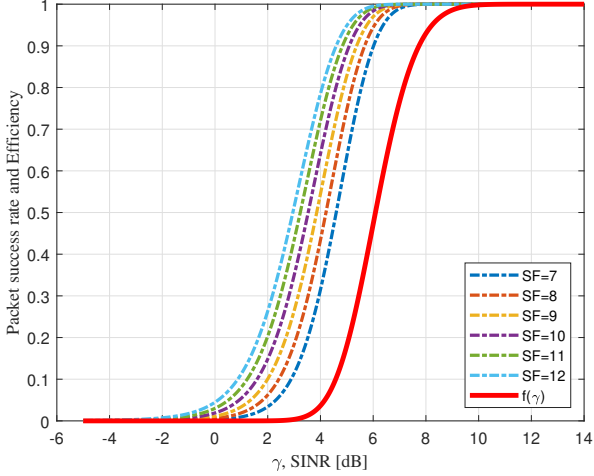


Fig. 2. The packet success rates of Multiple Frequency Shift Keying modulation (M-FSK) with different SF_k and the efficiency function versus SINR with $\alpha = 1$

- 3) $f' : (0, \infty) \rightarrow (0, f'_{max})$ for some finite constant $f'_{max} > 0$
- 4) $f'(\gamma^{SF_k}) \rightarrow \infty = \mathcal{O}((\gamma^{SF_k})^{-2})$

As CSS and M-FSK belong to the same modulation family (orthogonal modulations), they perform exactly the same over AWGN channel [27]. Fig. 2 demonstrates the PSR of coherence FSK for different SFs used in LoRaWAN over an AWGN channel, and the efficiency function proposed in Eq. (6).

It can be observed that the efficiency increases as a function of SINR, which is further determined by the transmit power p_i and the path gain h_i as $p_{rec,i} = P_i h_i$. Although increasing the transmission power of a node can improve the SINR and consequently the PSR, it comes at the cost of additional energy consumption and undue interference with other nodes. Therefore, a utility function is introduced to achieve a good balance between the packet success rate and the energy consumption. The utility function is defined as a ratio of the throughput to the transmit power, i.e.,

$$u_i^{SF_k}(p_i, \mathbf{p}_{-i}^{SF_k}) = \frac{R^{SF_k}(1 - 0.5e^{-\alpha\gamma_i^{SF_k}})L}{p_i} \frac{\text{bits}}{\text{Joule}}, \quad (7)$$

where $\mathbf{p}_{-i}^{SF_k} = [p_1, \dots, p_{i-1}, p_{i+1}, \dots, p_{M_k}]$ is the set of transmission powers of all nodes except node i using the same SF_k .

The transmit powers $\{p_i; i = 1, \dots, M_k\}$ can be optimized by following a distributed paradigm based on game theory.

B. Game Model

Each LoRa node aims to maximize its own utility function $u_i^{SF_k}$ to achieve a higher probability of packet success rate and to reduce the power consumption. Mathematically, it can be modeled by the expression of a basic game form in which LoRa nodes act as decision makers. LoRa nodes select their power level from a strategy power set. Thus, the basic power allocation game (normal form) can be expressed as:

$$\mathcal{G}^{SF_k} = \{\mathcal{M}^{SF_k}, \{\mathcal{P}_i^{SF_k}\}_{i=1}^{M_k}, \{u_i^{SF_k}\}_{i=1}^{M_k}(p_i, \mathbf{p}_{-i}^{SF_k})\} \quad (8)$$

where $\mathcal{M}^{SF_k} = 1, 2, \dots, M_k$ is the player set for each SF_k , $\mathcal{P}_i^{SF_k}$ is the i th player's power set, and $u_i^{SF_k}$ is the utility function defined in Eq. (7). In a distributed power allocation mechanism, each node uses only the local information to update its transmit power. The distributed power allocation can be implemented using a non-cooperative game theory, where the action of any node will affect the utility of all other nodes. The set of powers P^* resulting from the non-cooperative game is called Nash equilibrium at which no node acting alone can find a power level that increases its utility u_i^* when all nodes use P^* . At Nash Equilibrium, all nodes attain the same signal-to-interference and noise ratio $(\gamma_i^{SF_k})^*$, which is obtained by differentiating the utility function Eq. (7) with respect to the power p_i and setting the derivative equal to zero, i.e., $\partial u_i^{SF_k}(p_i, \mathbf{p}_{-i}^{SF_k}) / \partial p_i = 0$. The partial derivative of $u_i^{SF_k}(\cdot)$ with respect to p_i is given by [26], Appendix I:

$$\frac{\partial u_i^{SF_k}(p_i, \mathbf{p}_{-i}^{SF_k})}{\partial p_i} = \frac{1}{p_i^2} (f'_i(\gamma_i^{SF_k})(\gamma_i^{SF_k}) - f_i(\gamma_i^{SF_k})) \quad (9)$$

By setting the right side of Eq. (9) equal to zero, the value of $\gamma_i^{SF_k}$ represents the Nash equilibrium solution, i.e. $\frac{1}{p_i^2} (f'_i(\gamma_i^{SF_k})(\gamma_i^{SF_k}) - f_i(\gamma_i^{SF_k})) = 0$. Assuming that the efficiency function is given by Eq. (6) with $\alpha = 1$, and expressing $f'(\gamma_i^{SF_k})$ in terms of $f(\gamma_i^{SF_k})$, we get

$$\frac{L}{2}(\gamma_i^{SF_k}) + \frac{1}{2} = e^{(\gamma_i^{SF_k})} \quad (10)$$

It can be deduced that the right-hand side of the above equation is convex in $\gamma_i^{SF_k}$, and the left-hand side is monotonously increasing in $\gamma_i^{SF_k}$, and Eq. (10) is satisfied at $\gamma_i^{SF_k} = 0$. Therefore, there exists another positive value of $\gamma_i^{SF_k}$ that satisfies Eq. (10). It can be seen from Eq. (10) that this value is the same for all nodes for all SFs while assuming that all nodes operate with the same efficiency function. Let this value be $\gamma_i^{SF_k} = (\gamma^{SF_k})^* \forall k = 7, 8, \dots, 12$ which can be computed numerically from Eq. (10).

The Nash equilibrium resulting from Eq. (10) is inefficient because there is another set of power $P' < P^*$ which can generate higher utility for one or more nodes, without decreasing the utilities of other nodes. Some earlier works used price function as a solution to obtain a Pareto optimal [26], [28]. Despite the fact that price function can produce Nash equilibrium power where all nodes have higher utility, it leads to an inequitable equilibrium. In LoRaWAN and some energy-efficient technologies, using price function to optimize the transmit power is inefficient as it uses a gradient search procedure that exhibits slower convergence property than SINR balancing schemes [29]. Therefore, the SINR balancing method in LoRaWAN is introduced in this paper to offer practical and cheaper implementation. The proposed approach is referred to Best Equal LoRa (BE-LoRa).

V. BEST EQUAL SINR POWER ALLOCATION

As discussed previously, the Nash equilibrium achieved by maximizing the utility function of the game in Eq. (7) is inefficient because there exists another set of power that can achieve higher utility. Therefore, in this paper a power allocation scheme is proposed for LoRaWANs which requires

all the nodes operate with the same SINR. In this scheme, all LoRa nodes adjust their transmit power levels to attain the optimal solution $(\gamma^{\text{SF}_k})^{\text{opt}}$, which is computed at the network server for each SF. It depends on the number of active LoRa nodes and the processing gain of each SF. In the ADR algorithm, nodes update spreading factor and transmission power based on the channel condition (link-based adaptation), while the interference that depends on the number of nodes is not considered. For this reason, we consider the scenario where all LoRa nodes are assigned to SFs based on RSSI and a percentage and all nodes converge to an equilibrium set of power achieving the same $(\gamma^{\text{SF}_k})^T$.

A. The inefficient solution of Nash Equilibrium

It is known that there exists an $\epsilon < 1$ such that if all the nodes update their transmit power by that amount (with network cooperation), it will lead to an improvement on all nodes' utilities [29], [30]. The nodes' transmit powers were set to achieve an equal received power at the gateway. In [29], a condition of solution is given as $\gamma_i^\epsilon = \gamma_j^\epsilon, \forall i \neq j, \forall i, j \in M_k$, which means that all the received SINRs must be equal. This leads to nodes aiming for the same received power, $p_{rec,i} = p_{rec}, \forall i \in M_k$. Hence, the optimal SINR is $\gamma_i^\epsilon = (\gamma^{\text{SF}_k})^{\text{opt}}$

and the critical $\epsilon^* = \frac{(\frac{G_p^{\text{SF}_k}}{(\gamma^{\text{SF}_k})^*} - (M_k - 1))}{(\frac{G_p^{\text{SF}_k}}{(\gamma^{\text{SF}_k})^{\text{opt}}} - (M_k - 1))}$, where ϵ^* is unique.

The target SINR $(\gamma^{\text{SF}_k})^T$ guarantees that all LoRaWAN nodes operate with the same SINR and their signals received at the gateway have the same power level $p_{rec,i} = p_i h_i$. Thus, at the balanced SINR where $\gamma_i^{\text{SF}_k} = (\gamma^{\text{SF}_k})^T$, Eq. (4) can be rewritten as:

$$(\gamma^{\text{SF}_k})^T = \frac{G_p^{\text{SF}_k} p_{rec}^{\text{SF}_k}}{\sigma^2 + (M_k - 1) p_{rec}^{\text{SF}_k}} \quad (11)$$

and,

$$p_{rec}^{\text{SF}_k} = p_i h_i = \frac{(\gamma^{\text{SF}_k})^T \sigma^2}{G_p^{\text{SF}_k} - (M_k - 1) (\gamma^{\text{SF}_k})^T} \quad (12)$$

Whereas, the utility function in Eq. (7) can be rewritten with respect to $(\gamma^{\text{SF}_k})^T$ when the i th LoRa node achieves the target SINR $(\gamma^{\text{SF}_k})^T$:

$$\begin{aligned} u_i &= \frac{R^{\text{SF}_k} f((\gamma^{\text{SF}_k})^T) h_i [G_p^{\text{SF}_k} - (M_k - 1) (\gamma^{\text{SF}_k})^T]}{(\gamma^{\text{SF}_k})^T \sigma^2} \\ &= \frac{R^{\text{SF}_k} f((\gamma^{\text{SF}_k})^T) h_i \left[\frac{G_p^{\text{SF}_k}}{(\gamma^{\text{SF}_k})^T} - (M_k - 1) \right]}{\sigma^2} \end{aligned} \quad (13)$$

It can be seen from Eq. (13) that the target $(\gamma^{\text{SF}_k})^T$ affects utility for all nodes in the same way. It can also be seen that the utility of node i is a linear function of the path gain h_i , which is further determined by the node location. Similar to any spread spectrum technique, the feasibility of the system depends on the number of devices that can operate simultaneously. To ensure that the utility of node i is larger than 0, we can derive an upper bound for M_k , i.e. the maximum number of nodes that can simultaneously operate with $(\gamma^{\text{SF}_k})^T$ exists, which is given by,

$$M_k \leq 1 + \frac{G_p^{\text{SF}_k}}{(\gamma^{\text{SF}_k})^T} \quad (14)$$

From this feasibility condition, we can also interpret that in a LoRaWAN system with M_k nodes, there exists an upper bound on $(\gamma^{\text{SF}_k})^T$ that all M_k nodes can simultaneously achieve:

$$(\gamma^{\text{SF}_k})^T \leq \frac{G_p^{\text{SF}_k}}{M_k - 1} \quad (15)$$

The right hand side of Eq. (15) represents the ratio of processing gain to the number of interfering LoRa nodes in each SF. In this study, all LoRa nodes seek to maintain SINR value which produces optimum utility value as expressed by Eq. (7).

B. Necessary Conditions for Maximum

The utility maximization of transmission power for node i is equivalent to utility maximization of SINR. Thus, the utility maximization problem as advocated in [31] can be expressed as,

$$\max_{p_i} u_i = \max_{(\gamma^{\text{SF}_k})^T} \frac{R^{\text{SF}_k} f((\gamma^{\text{SF}_k})^T) h_i \left[\frac{G_p^{\text{SF}_k}}{(\gamma^{\text{SF}_k})^T} - (M_k - 1) \right]}{\sigma^2} \quad (16)$$

It is possible for the network server to find the optimum target SINR for each SF depending on the number of active nodes that are connected to the gateway. The network server computes the optimal target SINR by taking the derivative of utility function in Eq. (13) with respect to $(\gamma^{\text{SF}_k})^T$ and equating it to zero. The resulting differential equation is given by:

$$\left(1 - \frac{(\gamma^{\text{SF}_k})^T (M_k - 1)}{G_p^{\text{SF}_k}} \right) f'((\gamma^{\text{SF}_k})^T) (\gamma^{\text{SF}_k})^T = f((\gamma^{\text{SF}_k})^T) \quad (17)$$

The optimal target SINR $(\gamma^{\text{SF}_k})^{\text{opt}}$ is the solution to Eq. (17). It can be seen that the right hand side of Eq. (17) is positive because the value of the efficiency function $f(\cdot)$ given by Eq. (6) is positive. As $f(\cdot)$ is a monotonically increasing function, $f'((\gamma^{\text{SF}_k})^T) \geq 0 \forall (\gamma^{\text{SF}_k})^T \geq 0$. We thus obtain $\left(1 - \frac{(\gamma^{\text{SF}_k})^T (M_k - 1)}{G_p^{\text{SF}_k}} \right) \geq 0$. This implies that $0 \leq (\gamma^{\text{SF}_k})^T \leq \frac{G_p^{\text{SF}_k}}{M_k - 1}$ when $M_k > 1$. It indicates that there exists an optimal $(\gamma^{\text{SF}_k})^T = (\gamma^{\text{SF}_k})^{\text{opt}} \in \left[0, \frac{G_p^{\text{SF}_k}}{M_k - 1} \right]$ such that $u'((\gamma^{\text{SF}_k})^{\text{opt}}) = 0$. and it must be a maximum [32]. Moreover, with a constant value of $G_p^{\text{SF}_k}$, it is also noter from Eq. (17) that as M_k increases the target SINR $(\gamma^{\text{SF}_k})^T$ must decrease to compensate for the increase in M_k . In case of $M_k = 1$, $(\gamma^{\text{SF}_k})^{\text{opt}} = (\gamma^{\text{SF}_k})^*$ because Eq. (17) reduces to Eq. (10).

C. Uniqueness of the Solution

The optimum SINRs obtained by solving Eq. (17) are less than the respective values obtained by finding Nash equilibrium, i.e. $(\gamma^{\text{SF}_k})^{\text{opt}} < (\gamma^{\text{SF}_k})^*$, so we should only limit our search to $(\gamma^{\text{SF}_k})^{\text{opt}} \in [0, (\gamma^{\text{SF}_k})^*]$. Eq. (17) can be rewritten as follows

$$\left(1 - \frac{(\gamma^{\text{SF}_k})^T (M_k - 1)}{G_p^{\text{SF}_k}} \right) = \frac{f((\gamma^{\text{SF}_k})^T)}{f'((\gamma^{\text{SF}_k})^T) (\gamma^{\text{SF}_k})^T} \quad (18)$$

We know from [33] that the function

$$g((\gamma^{\text{SF}_k})^T) = f((\gamma^{\text{SF}_k})^T) - f'((\gamma^{\text{SF}_k})^T)(\gamma^{\text{SF}_k})^T \quad (19)$$

represents the y-intercept of the line tangent to $f((\gamma^{\text{SF}_k})^T)$ at the point $(\gamma^{\text{SF}_k})^T$. From the properties 1) and 2) of the efficiency function, the tangent line of $f((\gamma^{\text{SF}_k})^T)$ approaches to 1 when $(\gamma^{\text{SF}_k})^T \rightarrow \infty$, and hence $\lim_{(\gamma^{\text{SF}_k})^T \rightarrow \infty} g((\gamma^{\text{SF}_k})^T) = 1$. With the property 4) of the efficiency sigmoid function, this implies that $\lim_{(\gamma^{\text{SF}_k})^T \rightarrow \infty} (\gamma^{\text{SF}_k})^T f'((\gamma^{\text{SF}_k})^T) = 0$.

Given that $g(0) = 0$ and $g((\gamma^{\text{SF}_k})^T) < 0, \forall (\gamma^{\text{SF}_k})^T \in (0, (\gamma^{\text{SF}_k})^*)$, we can get

$$\frac{f((\gamma^{\text{SF}_k})^T)}{(\gamma^{\text{SF}_k})^T f'((\gamma^{\text{SF}_k})^T)} \leq 1, \quad \forall (\gamma^{\text{SF}_k})^T \in [0, (\gamma^{\text{SF}_k})^*] \quad (20)$$

Given aforementioned general properties of the efficiency function $f((\gamma^{\text{SF}_k})^T)$ in section IV, we find an additional property as follows:

Property 5): $h((\gamma^{\text{SF}_k})^T) \equiv \frac{f((\gamma^{\text{SF}_k})^T)}{(\gamma^{\text{SF}_k})^T f'((\gamma^{\text{SF}_k})^T)}$ is convex [32].

Proposition 1: Given that $h((\gamma^{\text{SF}_k})^T)$ is convex for $(\gamma^{\text{SF}_k})^T \in (0, (\gamma^{\text{SF}_k})^*)$, there exist values $(\gamma^{\text{SF}_k})^{\text{opt}} \in (0, (\gamma^{\text{SF}_k})^*)$ such that Eq. (17) is satisfied if and only if $h'(0) < -(M_k - 1)/G_p^{\text{SF}_k}$. Further, $(\gamma^{\text{SF}_k})^{\text{opt}}$ are the values which maximize Eq. (13) for each SF.

Proof: As in [32], the left hand side (LHS) of Eq. (18) is a decreasing line with slope $-(M_k - 1)/G_p^{\text{SF}_k}$. The function $h((\gamma^{\text{SF}_k})^T)$ is the right hand side (RHS) of Eq. (18). If $h'(0) < -(M_k - 1)/G_p^{\text{SF}_k}$, since $h((\gamma^{\text{SF}_k})^T)$ is convex, the value of $h((\gamma^{\text{SF}_k})^T)$ must eventually start increasing. Since $h((\gamma^{\text{SF}_k})^T)$ never takes values less than zero, there must be a non-zero point where the curves of LHS and RHS of Eq. (18) intersect, as shown in Fig. (3). Conversely, if $h'(0) \geq -(M_k - 1)/G_p^{\text{SF}_k}$, as $h((\gamma^{\text{SF}_k})^T)$ is convex it will never intersect the line with a slope $-(M_k - 1)/G_p^{\text{SF}_k}$. Since a solution does exist and it is greater than zero, we end up with a contradiction. Therefore, we can conclude that $h'(0) < -(M_k - 1)/G_p^{\text{SF}_k}$. As the only other solution to Eq. (17) is 0 and we know that it does not lead to a maximum, we conclude that $(\gamma^{\text{SF}_k})^{\text{opt}}$ is the maximum and it is the only non-zero solution to Eq. (17).

D. Feasibility of $(\gamma^{\text{SF}_k})^{\text{opt}}$

To find that the obtained values $(\gamma^{\text{SF}_k})^{\text{opt}}$ are indeed feasible, Eq. (4) can be rewritten as:

$$\gamma_i^{\text{SF}_k} = \frac{G_{p,i}^{\text{SF}_k} p_{\text{rec},i}}{\sigma^2 + \sum_{j=1, j \neq i}^{M_k} p_{\text{rec},j}} = G_{p,i}^{\text{SF}_k} (CIR_i) \quad (21)$$

where CIR_i is the carrier-to-interference and noise ratio. The feasibility constraint obtained from [32] are

$$\sum_{i=1}^{M_k} \frac{CIR_i}{CIR_i + 1} < 1 \quad \text{if } \sigma^2 > 0 \quad (22)$$

and

$$\sum_{i=1}^{M_k} \frac{CIR_i}{CIR_i + 1} = 1 \quad \text{if } \sigma^2 = 0 \quad (23)$$

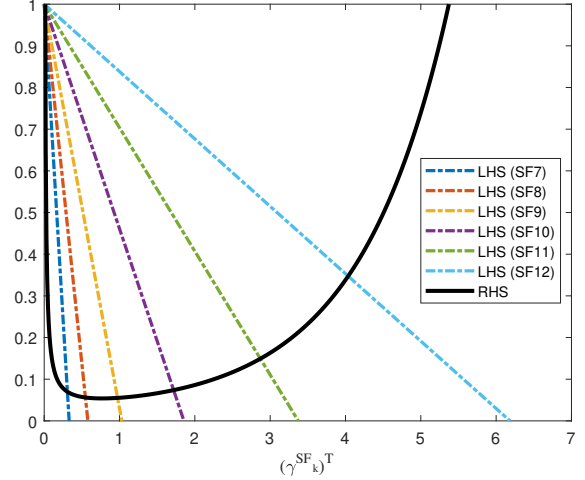


Fig. 3. Left hand side and right hand side of Eq. (18) with different values of SF.

We consider the scenario where $\sigma^2 > 0$. Since all the M_k nodes in $\text{SF}_k \forall k = 7, 8, \dots, 12$, have the same processing gain based on Eq. (3), and all of them achieve the maximum utility at $(\gamma^{\text{SF}_k})^T = (\gamma^{\text{SF}_k})^{\text{opt}}$, Eq. (22) can be rewritten as

$$\sum_{i=1}^{M_k} \frac{(\gamma^{\text{SF}_k})^{\text{opt}}}{(\gamma^{\text{SF}_k})^{\text{opt}} + G_p^{\text{SF}_k}} < 1 \quad (24)$$

It can be further deduced that

$$(\gamma^{\text{SF}_k})^{\text{opt}} < \frac{G_p^{\text{SF}_k}}{M_k - 1} \quad \forall k = 7, 8, \dots, 12 \quad (25)$$

which is identical to the feasibility constraint given in Eq. (15).

E. Pareto Optimality of BE-LoRa

In the proposed work, Pareto optimal solution as described in [26] is modified to conform with BE-LoRa problem formulation.

Theorem 1: A vector $\overrightarrow{(\gamma^{\text{SF}_k})^*}(\overrightarrow{\beta})$ that solves the social problem given by Eq. (25) is Pareto optimal with $\overrightarrow{\beta}$ being a vector of positive scalars, $\beta_i > 0, \forall \beta_i \in \overrightarrow{\beta}$. Further, the solution exists, is unique and independent of β_i

$$\begin{aligned} & \max_{\gamma_i^{\text{SF}_k}} \sum_i^{M_k} \beta_i u_i \\ &= \max_{\gamma_i^{\text{SF}_k}} \sum_i^{M_k} \beta_i \frac{R^{\text{SF}_k} f((\gamma^{\text{SF}_k})^T) h_i}{\sigma^2} \left[\frac{G_p^{\text{SF}_k}}{(\gamma^{\text{SF}_k})^T} - (M_k - 1) \right] \\ &= \max_{\gamma_i^{\text{SF}_k}} \left(\sum_i^{M_k} \beta_i \frac{h_i}{\sigma^2} \right) R^{\text{SF}_k} f((\gamma^{\text{SF}_k})^T) \left[\frac{G_p^{\text{SF}_k}}{(\gamma^{\text{SF}_k})^T} - (M_k - 1) \right] \end{aligned} \quad (26)$$

Proof: The maximum of $R^{\text{SF}_k} f((\gamma^{\text{SF}_k})^T) \left[\frac{G_p^{\text{SF}_k}}{(\gamma^{\text{SF}_k})^T} - (M_k - 1) \right]$ is independent of β_i . Since we have proved that $f((\gamma^{\text{SF}_k})^T) \left[\frac{G_p^{\text{SF}_k}}{(\gamma^{\text{SF}_k})^T} - (M_k - 1) \right]$ has a unique maximum the proof is complete. The reason that the solution is independent

of β_i 's is because the users have already agreed to operate at equal received powers.

VI. BEST EQUAL-SINR ALGORITHM

The BE-LoRa power allocation algorithm operates to maintain the SINR of each LoRa node above the target SINR. The maximum number of LoRa nodes in each SF can be computed using Eq. (14) while considering the target SINR for all LoRa nodes to be $\Gamma = 6\text{dB}$.

Eq. (17) is solved to find the optimal target SINR for each SF given the number of LoRa nodes. Fig. 4 shows the optimum target SINR versus the number of nodes for different SFs. The crossing points of colored curves with the dashed black line (SINR target Γ_i) represent the maximum number of LoRaWAN nodes in each SF that can operate simultaneously. Fig. 4 can assist with determining the best target SINR set $[(\gamma^{\text{SF}_7})^{\text{opt}}, (\gamma^{\text{SF}_8})^{\text{opt}}, \dots, (\gamma^{\text{SF}_{12}})^{\text{opt}}]$ when the number of simultaneous LoRa nodes in each SF is smaller than the maximum number at the crossing point. Accordingly, the optimum number of simultaneous LoRa nodes in each SF can be used by the network server for SF assignment. The percentages are summarized in Table III for BE-LoRa algorithm.

TABLE III
PERCENTAGE OF NODES ASSIGNED TO EACH SPREADING FACTOR IN BE-LORA.

Spreading factor	7	8	9	10	11	12
No of nodes at Γ	4	7	12	22	39	72
Percentage of nodes %	2.56	4.49	7.69	14.1	25	46.15

The BE-LoRa algorithm is running on a network server which is capable of changing the transmission power and assigning end nodes to a certain SF. The database at the network server contains the list of all nodes with the last RSSIs, and the network server is able to sort this list of nodes based on RSSI in descending order (from the highest RSSI to the lowest). Then, the network server assigns the SFs to the nodes based on the percentages provided in Table III. It also estimates the SNR from the received frames at gateway and gets the maximum value of the last 20 records to compare it with the optimal SINR. In the BE-LoRa algorithm, 1dB margin is used between the optimal SINR and the maximum SINR to stop updating the power within this margin. The network server decreases (or increases) the transmission power by 1 dBm when the max SINR is greater (or less) than the optimal SINR plus 1dB. The newly calculated SF and transmit power are transmitted to a LoRa node through a downlink frame. The LoRa node updates its SF and transmission power settings according to the settings received from the network server and uses these new settings for the following transmissions.

Finding the optimal SINRs for each SF, assigning SF, and updating transmission power of nodes are summarized in algorithm 1.

VII. PERFORMANCE EVALUATION

In this section, we evaluate the performance of the proposed BE-LoRa power allocation algorithm. We will first use Matlab

Algorithm 1: Network Server BE-LoRa Algorithm

Input: List of LoRa nodes M , processing gain for each SF, $G_p^{\text{SF}_k}$, corresponding RSSIs, initial transmission power=14 dBm, initial spreading factors=12.

Output: The optimal target SINR for each SF, updated transmit power, updated SF assignment for all nodes.

- 1: Sort the LoRa nodes M in descending Order of RSSI
 - 2: **for** $i = 1$ to M **do**
 - 3: Assign node i with a SF based on the percentage in Table III
 - 4: **end for**
 - 5: Find the optimal target SINR $(\gamma^{\text{SF}_k})^{\text{opt}}$ for each SF by solving Eq. (17).
 - 6: **if** $(\gamma^{\text{SF}_k})^{\text{opt}} < \Gamma_i$ **then**
 - 7: $(\gamma^{\text{SF}_k})^{\text{opt}} = \Gamma_i$;
 - 8: **end if**
 - 9: **for** $i = 1$ to M **do**
 - 10: $\gamma_i^{\text{SF}_k} = \max(\text{SNR of last 20 frames})$
 - 11: **if** $\gamma_i^{\text{SF}_k} > ((\gamma^{\text{SF}_k})^{\text{opt}} + 1\text{dB})$ **then**
 - 12: $p_i = p_i - 1\text{dBm}$
 - 13: **else if** $(\gamma_i^{\text{SF}_k} < ((\gamma^{\text{SF}_k})^{\text{opt}} - 1\text{dB}))$ **then**
 - 14: $p_i = p_i + 1\text{dBm}$
 - 15: **else**
 - 16: Break;
 - 17: **end if**
 - 18: **end for**
-

to perform numerical evaluation, and then simulate the BE-LoRa algorithm in a discrete event network simulator OMNET++ based on FLoRa framework. The numerical results will be compared with the simulation results in terms of average transmissions power. The simulation results of BE-LoRa and LoRaWAN ADR algorithms are also compared in terms of network delivery ratio and energy consumption.

A. Experimental setup

The LoRaWAN ADR algorithm has two parts, one running at the network server and the other at the LoRa nodes. The algorithm at network server part is able to change the transmission power and the SF for the uplink data transmissions of end nodes. By estimating the link budget of each node using the SNR of received frames, the network server updates the transmission parameters based on the knowledge of the minimum SNR (SNRreq) required for demodulation, which is adjusted by a device-specific margin. These updates of transmission parameters are sent to the nodes via downlink frame and nodes use these settings for transmissions [34]. The network server does not increase the SF, as this is done by the other part of the LoRaWAN ADR algorithm at LoRa node. The initial spreading factor and transmission power for all nodes are set to be 12 and 14 dBm respectively. The gateway is located at the centre of the network and connected to one network server. LoRa nodes are distributed uniformly over the deployment area and the European regional parameters for the LoRa physical layer detailed in Table IV are used. The simulation time is 12 days for each individual experiment and

the simulations included a warm-up period of 2 days. We run 10 iterations of each experiment (BE-LoRa and LoRaWAN ADR) according to the independent replication method in OMNET++. The plots show the average value obtained over all replications. The other network parameters follow the specifications given in [34].

The number of LoRa nodes considered for the analysis are 156 nodes, which are equal to the total number of nodes at the target SINR Γ_i . The efficiency function and a comparison between numerical and simulation results is presented. Next, the delivery ratio, energy consumed, transmit power and number of ADR commands are estimated in each SF when the number of nodes is 624. Finally, the performance in terms of delivery ratio, energy consumed, and number of collisions is compared for varying number of nodes, i.e., {156, 312, 468, 612}.

The LoRaWAN ADR algorithm estimates the link quality using the maximum SNR value of the past 20 records. This is ideal when there is no variability in the channel quality. It is assumed that both algorithms operate in the channel condition where the standard deviation of the path loss is assumed to be 0dB; otherwise some transmissions might not be able to reach the destination, rendering the results inconclusive [34].

The common system parameters that are used in the evaluation are summarized in Table IV.

TABLE IV
LIST OF SYSTEM PARAMETERS USED IN EVALUATION.

System Parameters	
L , Information bits per frame	80
α , a constant that depends on the system modulation	1
Bandwidth (BW)	125 KHz
Additive White Gaussian noise σ^2	3.2×10^{-15}
Frequency (f)	868 MHz
Target SINR (Γ_i)	6 dB
Network size	480m X 480m
Transmission Power	2 dBm to 14 dBm
Spreading factor	7 to 12
Code Rate	4/5

B. Efficiency function

The results presented in Fig. 4 indicate that the higher the number of active nodes in the network, the lower the optimum target SINR. To show the impact of network scale on the system efficiency, the efficiency function as defined in Eq. (6) is computed against the varying number of nodes in each SF M_k . Fig. 5 plots the efficiency functions for different SFs. It is shown that for each SF, the efficiency function increases with the increasing number of nodes until the maximum point where all the nodes of that SF achieve the optimum target SINR Γ_i . The efficiency function starts to decrease when the number of nodes in a LoRaWAN is more than the optimum number. These results are significant from a network designer's perspective, where the system efficiency can be identified for a particular SF and the number of LoRaWAN nodes.

C. Comparison between average transmission power numerical evaluation and simulation

The BE-LoRa algorithm is evaluated using both MATLAB and OMNET++ with the same parameter settings. The results

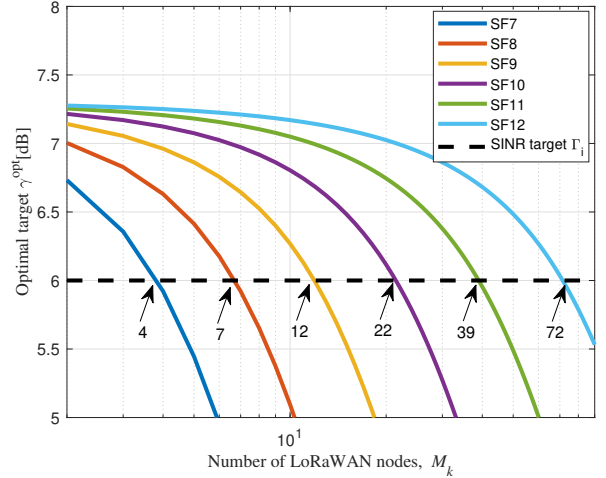


Fig. 4. Optimum target SINR as a function of the number of LoRa nodes simultaneously transmitting with different spreading factors.

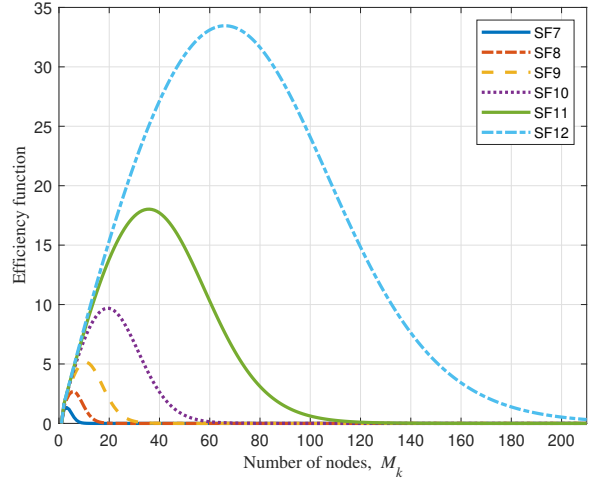


Fig. 5. The efficiency function versus the number of LoRaWAN nodes for different SFs

are compared in terms of the average transmission power in each SF. In the evaluation, we consider a LoRaWAN with 156 nodes randomly distributed at fixed distances from the gateway that is located at the cell center. All nodes are assigned with a SF based on the percentages presented in Table III. The transmission powers of nodes in the numerical evaluation were computed by solving (16). Fig. 6 plots the average transmission powers for all SFs obtained by both numerical evaluation and simulation. It can be observed that the numerical evaluation results match the simulation results with small errors in some SFs (i.e. SF7 and SF10) due to the round function that is applied to find the nearest average transmission power in each SF.

D. Comparison between BE-LoRa and legacy ADR

In this section, we present the performance of the proposed BE-LoRa power allocation algorithm by comparing it with the legacy ADR scheme as specified in the LoRaWAN standard.

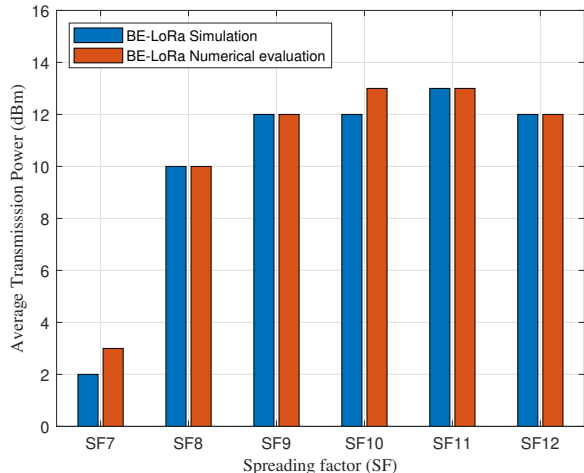


Fig. 6. Average transmission powers obtained by numerical evaluation and simulation.

We consider a LoRa network with 624 Class A nodes and the two algorithms are compared in terms of delivery ratio, energy consumption per successful transmission, average node transmit power and convergence speed. The state-based energy consumer module in FLoRa is used to model the energy expenditure of LoRa nodes. It computes the energy consumed depending on the time spent by the LoRa radio in the main three states: transmit, receive and sleep state [34]. The energy consumed in the transmit state depends on the values of instantaneous current of each transmission power level [12]. The sleep state occurs after transmitting or receiving a frame and the current drawn during the receive and sleep modes are derived from the Semtech SX1272/73 datasheet with a supply voltage of 3.3 V [35].

1) *SF assignment*: Fig. 7 shows the number of nodes in each SF for both BE-LoRa and ADR schemes. In the legacy LoRaWAN ADR, assignment of SFs to the nodes is based on the link budget between the node and the gateway. One of the disadvantages of updating SF in LoRaWAN ADR algorithm is that if all nodes are located equidistant from the gateway, one SF will be assigned to all nodes. On the other hand, the SF assignment in BE-LoRa is aligned with the breakdown in Table IV. The SFs are assigned to the nodes based on the optimal SINRs, which guarantees that all nodes achieve these optimal values using a minimal transmission power. It is shown in Fig. 7 that BE-LoRa decreased the number of nodes in SF7, SF11 and SF12 while increasing the number of nodes in the other SFs (SF8, SF9, and SF10). Efficient assignment of SFs in the BE-LoRa algorithm leads to less collisions (increased packet delivery ratio) and improves the energy consumption. Moreover, increasing the number of nodes in one SF leads to more collisions as shown in SF12 of ADR LoRaWAN compared with the BE-LoRa algorithm.

2) *Delivery ratio*: Next, we compare the two algorithms in terms of delivery ratio. The delivery ratio is computed as the number of successful packets received by the network server divided by the number of packets sent by all LoRa nodes. Fig. 8 shows the delivery ratios for the BE-LoRa algorithm

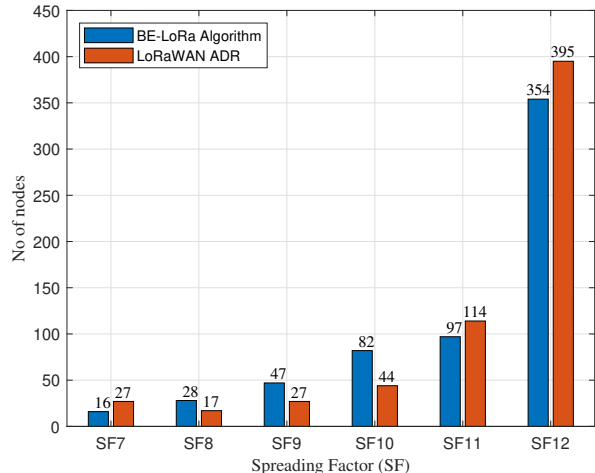


Fig. 7. SF assignment in LoRaWAN ADR and BE-LoRa algorithms

and the LoRaWAN ADR algorithm. It can be observed that the delivery ratio of BE-LoRa is higher than LoRaWAN ADR for all SFs. The delivery ratio declines with the increase in SF index number. This is because nodes assigned with a higher SF are located farther from the gateway and hence suffer from higher channel error rates. It can be also seen that the BE-LoRa algorithm offers a significant improvement when SF increases.

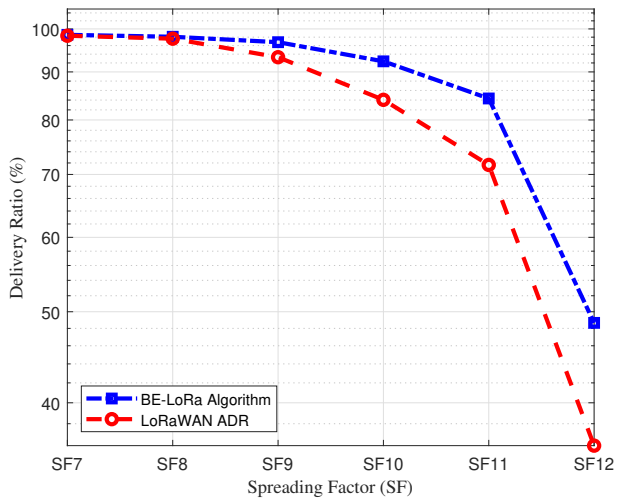


Fig. 8. Delivery ratio comparison between BE-LoRa and LoRaWAN ADR

3) *Energy consumption*: Fig. 9 plots the energy consumption per successful transmission for both algorithms. The energy consumption is computed as the total energy consumed by all LoRa nodes divided by the number of packets successfully received by the network server. It can be observed that BE-LoRa provides a significant decrease in the energy consumption for all SFs. For example, if we observe at SF12, the energy consumed for BE-LoRa algorithm is 500 mJ, while the energy consumed for LoRaWAN ADR is 800 mJ. These results highlight the performance gains achieved by the proposed

BE-LoRa algorithm in terms of energy consumption. This is

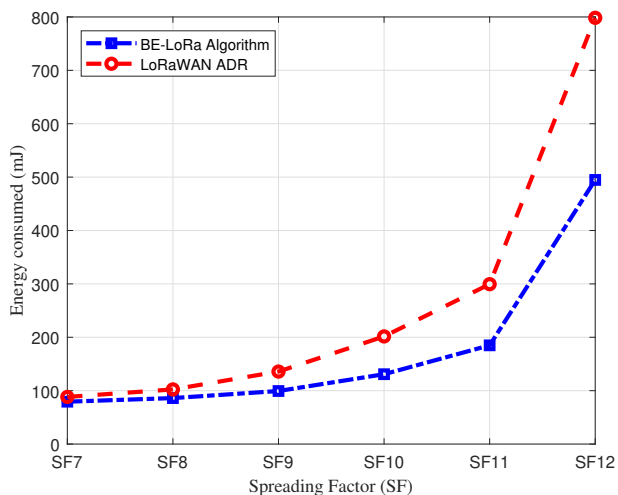


Fig. 9. Energy consumption comparison between BE-LoRa and LoRaWAN ADR

because all of the nodes in the BE-LoRa algorithm achieve the optimal target SINR which maximizes the utility function defined in Eq. (13). Compared to the legacy LoRaWAN ADR, BE-LoRa is more energy-efficient. The average transmit power of nodes in each SF is compared in Fig. 10. It can be seen that in LoRaWAN ADR all the nodes between SF8 - SF12 operate at the maximum transmit power of 14dBm. Referring to the SF assignment results in Fig. 7, 93% of the nodes in LoRaWAN ADR operate at 14dBm. However, in BE-LoRa even the highest transmit power is lower than 14dBm, and the percentage of nodes operating at this highest transmit power (13dBm) is only 47%. These results signify the performance gains that can be achieved by the proposed algorithm.

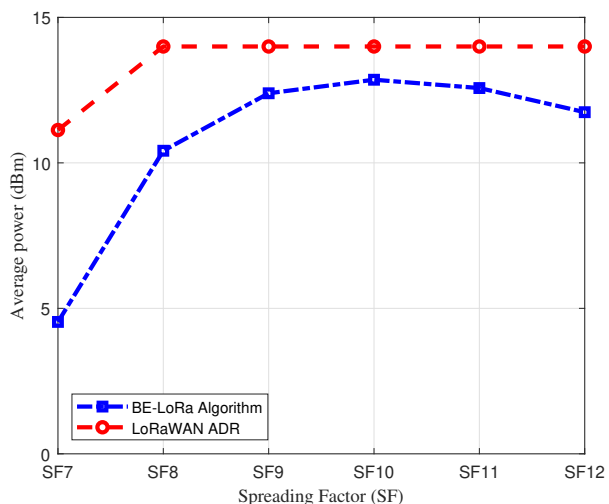


Fig. 10. Comparison of average transmit power of nodes between BE-LoRa and LoRaWAN ADR.

4) *Convergence speed*: Next, we compare the speed of convergence for the two algorithms, i.e. the time it takes to

reach an equilibrium. In OMNET++ simulation, we cannot record this convergence time. Instead we use the average number of communication commands exchanged between the network server and each node to evaluate the convergence speed. The fewer the communication commands exchanged, the faster the algorithm converges. In LoRaWAN ADR, the system reaches the equilibrium by completing no of steps equal to $\text{floor}(SNR_{margin}/3)$, while in BE-LoRa the equilibrium is reached when all nodes achieve the optimal SINR plus a margin. Fig. 11 shows the average number of ADR commands received by a node to reach the equilibrium versus the SF. It is shown that BE-LoRa algorithm and LoRaWAN ADR algorithm requires approximately the same number of ADR commands to reach the equilibrium.

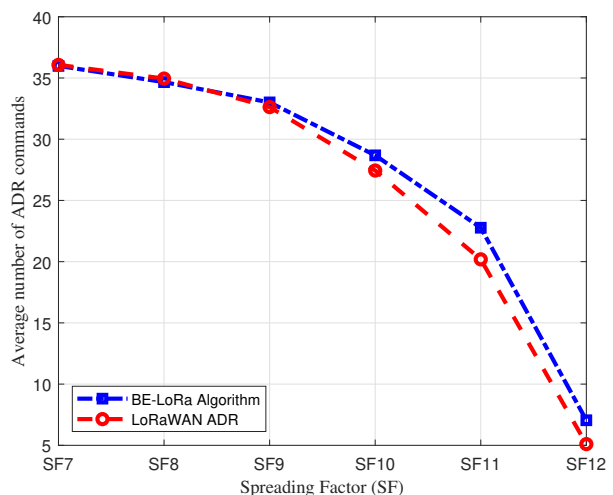


Fig. 11. Comparison of average number of ADR commands received by a node between BE-LoRa and LoRaWAN ADR in each SF.

5) *Impact of network density*: To further illustrate the improvement that the proposed BE-LoRa algorithm can offer as compared to the LoRaWAN ADR, we studied the performance at different network scale, i.e., 156, 312, 468, and 624 nodes distributed in the same geographic area. The delivery ratio and energy consumption is examined for both algorithms.

Fig. 12 shows that the delivery ratio decreases with the increase in the number of nodes for both BE-LoRa and LoRaWAN ADR algorithms, as the number of nodes increases from 150 to 624. This is expected as more nodes result in higher co-SF interference and more collisions. The packet delivery ratio for the proposed scheme is higher than the LoRaWAN ADR. For example, for no of nodes= 156, the packet delivery ratio of BE-LoRa is 91.13 %, while the packet delivery ratio of LoRaWAN ADR is 85.73 %. The difference in packet delivery ratio increases when the number of nodes increases, e.g., when no of nodes = 624, the packet delivery in BE-LoRa is 68.29 % and in LoRaWAN ADR is 53.82%.

Fig. 13 shows the energy consumption per successful transmission versus the number of nodes in the network. Compared to LoRaWAN ADR, the energy consumption in BE-LoRa is much lower. BE-LoRa saves energy in mJ by 32% with 156 nodes and 46% when the number of nodes is increased up

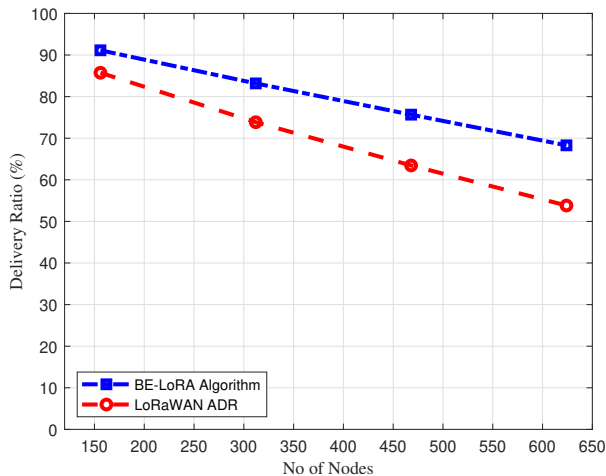


Fig. 12. Delivery ratio comparison between BE-LoRa and LoRaWAN ADR with different number of nodes.

to 624. This indicates the benefit that BE-LoRa can offer in terms of energy efficiency, especially for larger networks.

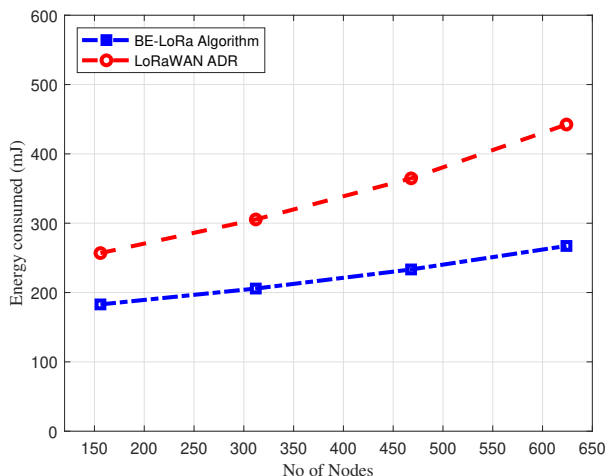


Fig. 13. Energy consumption comparison between BE-LoRa and LoRaWAN ADR with different number of nodes.

Fig. 14 shows the number of collisions occurring in the network for different network scales. It can be seen that the number of collisions increases with the increase in the number of nodes. Moreover, the number of collisions for BE-LoRa is lower than the the number of collisions observed for LoRaWAN ADR, thereby highlighting the superior performance of the proposed algorithm. The LoRaWAN ADR algorithm can improve the link budget by updating the spreading factor and transmission power for each link, but this approach does not take into consideration the interference caused by transmission from the same SF. This interference can significantly decrease delivery ratio in dense networks. On the other hand, the BE-LoRa algorithm is based on the best equal SINR game model in which the number of nodes is constrained in each SF based on the target SINR and the processing gains. The optimal SINRs are slightly decreased by increasing the number of

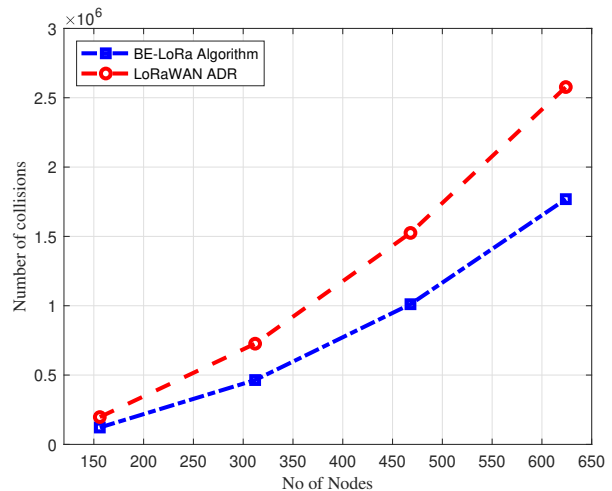


Fig. 14. Number of collisions occur in BE-LoRa algorithm and LoRaWAN ADR with different number of nodes, 156,312,468, 624 nodes.

nodes until reaching the target. The BE-LoRa algorithm leads the nodes to an appropriate choice of SF and guides them to transmit at lowest possible power to achieve these optimal SINRs.

VIII. CONCLUSION

In this paper, the power allocation problem for uplink communication in the long-range IoT networks has been investigated using game theory. We propose a best equal algorithm, which is a cooperation power allocation where the LoRa nodes behave in a fashion consistent with the information that the network server provides. This paper demonstrates the fair solution of equal received power that leads to maximizing the node packet delivery ratio and energy efficiency. We have shown that there exists an optimal solution and it is unique for each SF. We have also shown the effectiveness of BE-LoRa, which comes about from the assumption that the received signal strengths from all LoRa nodes are equal. The BE-LoRa algorithm is based on the number of nodes in each SF in which the interference is considered, and the optimal SINR that nodes should achieve is slightly reduced by increasing the number of nodes. Our simulation results showed that BE-LoRa has a higher delivery ratio and lower energy consumption compared with LoRaWAN ADR. Admission algorithm together with BE-LoRa at the network server to limit the number of LoRaWAN nodes in each SF is one of the future research directions of this work.

ACKNOWLEDGMENT

We thank the University of Northumbria and Cara for their support.

REFERENCES

- [1] "sigfox," 2016. [Online]. Available: <http://www.sigfox.com>.
- [2] S. Landström, J. Bergström, E. Westerberg, and D. Hammarwall, "NB-IoT: A sustainable technology for connecting billions of devices," *Ericsson Technology Review*, vol. 4, pp. 2–11, 2016.

- [3] “weightless,” jan 2018. [Online]. Available: <http://www.weightless.org/>
- [4] N. Sornin, M. Luis, T. Eirich, T. Kramp, and O. Hersent, “LoRaWAN™ 1.0 Specification,” <http://www.lora-alliance.org>, jan 2015.
- [5] Link-Labs, “A Comprehensive Look at Low Power, Wide Area Networks for Internet of Things Engineers and Decision Makers,” 2016.
- [6] B. Reynders, W. Meert, and S. Pollin, “Power and spreading factor control in low power wide area networks,” in *2017 IEEE International Conference on Communications (ICC)*. IEEE, 2017, pp. 1–6.
- [7] B. Reynders, Q. Wang, P. Tuset-Peiro, X. Vilajosana, and S. Pollin, “Improving reliability and scalability of lorawans through lightweight scheduling,” *IEEE Internet of Things Journal*, vol. 5, no. 3, pp. 1830–1842, 2018.
- [8] J. Haxhibeqiri, I. Moerman, and J. Hoebeke, “Low overhead scheduling of LoRa transmissions for improved scalability,” *IEEE Internet of Things Journal*, vol. 6, no. 2, pp. 3097–3109, 2018.
- [9] O. Georgiou and U. Raza, “Low power wide area network analysis: Can LoRa scale?” *IEEE Wireless Communications Letters*, vol. 6, no. 2, pp. 162–165, 2017.
- [10] K. Q. Abdelfadeel, V. Cionca, and D. Pesch, “Fair adaptive data rate allocation and power control in lorawan,” in *2018 IEEE 19th International Symposium on A World of Wireless, Mobile and Multimedia Networks (WoWMoM)*, 2018, pp. 14–15.
- [11] B. Reynders, W. Meert, and S. Pollin, “Range and coexistence analysis of long range unlicensed communication,” in *2016 23rd International Conference on Telecommunications (ICT)*. IEEE, 2016, pp. 1–6.
- [12] M. C. Bor, U. Roedig, T. Voigt, and J. M. Alonso, “Do LoRa low-power wide-area networks scale?” in *Proceedings of the 19th ACM International Conference on Modeling, Analysis and Simulation of Wireless and Mobile Systems*. ACM, 2016, pp. 59–67.
- [13] F. den Abeele, J. Haxhibeqiri, I. Moerman, and J. Hoebeke, “Scalability analysis of large-scale LoRaWAN networks in ns-3,” *IEEE Internet of Things Journal*, vol. 4, no. 6, pp. 2186–2198, 2017.
- [14] D. Magrin, M. Centenaro, and L. Vangelista, “Performance evaluation of LoRa networks in a smart city scenario,” in *2017 IEEE International Conference on Communications (ICC)*. IEEE, 2017, pp. 1–7.
- [15] D. Croce, M. Gucciardo, S. Mangione, G. Santaromita, and I. Tinnirello, “Impact of LoRa imperfect orthogonality: Analysis of link-level performance,” *IEEE Communications Letters*, vol. 22, no. 4, pp. 796–799, 2018.
- [16] A. Mahmood, E. Sisinni, L. Guntupalli, R. Rondón, S. A. Hassan, and M. Gidlund, “Scalability analysis of a LoRa network under imperfect orthogonality,” *IEEE Transactions on Industrial Informatics*, vol. 15, no. 3, pp. 1425–1436, 2018.
- [17] V. Sharma, G. Choudhary, I. You, J. D. Lim, and J. N. Kim, “Self-enforcing game theory-based resource allocation for LoRaWAN assisted public safety communications,” *Journal of Internet Technology*, vol. 19, no. 2, pp. 515–530, 2018.
- [18] O. Seller and N. Sornin, “Low power long range transmitter,” *US Patent 20140219329 A*, vol. 1, 2014.
- [19] L. Alliance, “LoRaWAN™ 1.0.3 Regional Parameters,” 2018.
- [20] F. Adelantado, X. Vilajosana, P. Tuset-Peiro, B. Martinez, J. Melia-Segui, and T. Watteyne, “Understanding the limits of LoRaWAN,” *IEEE Communications magazine*, vol. 55, no. 9, pp. 34–40, 2017.
- [21] A. Lavric and V. Popa, “Performance evaluation of LoRaWAN communication scalability in large-scale wireless sensor networks,” *Wireless Communications and Mobile Computing*, vol. 2018, 2018.
- [22] S. Li, U. Raza, and A. Khan, “How Agile is the Adaptive Data Rate Mechanism of LoRaWAN?” in *2018 IEEE Global Communications Conference (GLOBECOM)*, 2018, pp. 206–212.
- [23] T. S. Rappaport *et al.*, *Wireless communications: principles and practice*. prentice hall PTR New Jersey, 1966.
- [24] A. Semtech, “120022,” *LoRa Modulation Basics*, 2015.
- [25] C. Goursaud and J.-M. Gorce, “Dedicated networks for IoT: PHY/MAC state of the art and challenges,” *EAI Endorsed Transactions on Internet of Things*, 2015.
- [26] C. U. Saraydar, N. B. Mandayam, D. J. Goodman, and Others, “Efficient power control via pricing in wireless data networks,” *IEEE transactions on Communications*, vol. 50, no. 2, pp. 291–303, 2002.
- [27] A. Marquet, N. Montavont, and G. Z. Papadopoulos, “Towards an SDR implementation of LoRa: Reverse-engineering, demodulation strategies and assessment over Rayleigh channel,” *Computer Communications*, vol. 153, pp. 595–605, 2020.
- [28] Y. Al-Gumaei, K. Noordin, A. Reza, and K. Dimiyati, “A novel utility function for energy-efficient power control game in cognitive radio networks,” *PLoS ONE*, vol. 10, no. 8, 2015.
- [29] D. Goodman and N. Mandayam, “Network assisted power control for wireless data,” *Mobile Networks and Applications*, vol. 6, no. 5, pp. 409–415, 2001.
- [30] A. B. MacKenzie and S. B. Wicker, “Game theory in communications: Motivation, explanation, and application to power control,” in *GLOBECOM’01. IEEE Global Telecommunications Conference (Cat. No. 01CH37270)*, vol. 2, 2001, pp. 821–826.
- [31] G. Alyfantis, S. Hadjiefthymiades, and L. Merakos, “On fair and efficient power control in cdma wireless data networks,” in *Proceedings of 15th International Conference on Computer Communications and Networks*, 2006, pp. 309–314.
- [32] Z. Marantz, “On the optimality of network assisted power control for a general class of sigmoid functions,” in *2013 Wireless Telecommunications Symposium (WTS)*. IEEE, 2013, pp. 1–5.
- [33] V. Rodriguez, “An analytical foundation for resource management in wireless communication,” in *GLOBECOM’03. IEEE Global Telecommunications Conference (IEEE Cat. No. 03CH37489)*, vol. 2. IEEE, 2003, pp. 898–902.
- [34] M. Slabicki, G. Premsankar, and M. Di Francesco, “Adaptive configuration of lora networks for dense IoT deployments,” *IEEE/IFIP Network Operations and Management Symposium: Cognitive Management in a Cyber World, NOMS 2018*, pp. 1–9, 2018.
- [35] D. Bankov, E. Khorov, and A. Lyakhov, “On the limits of lorawan channel access,” in *2016 International Conference on Engineering and Telecommunication (EnT)*. IEEE, 2016, pp. 10–14.



2010. His research interests include resource allocations in wireless networks, game theory, and Internet of things, 5G.



Nauman Aslam (Member, IEEE) received the Ph.D. degree in engineering mathematics from Dalhousie University, Halifax, NS, Canada, in 2008, where he was an Assistant Professor. He is currently a Professor with the Department of Computer and Information Sciences, Northumbria University, Newcastle upon Tyne, U.K. He is also an Adjunct Assistant Professor with Dalhousie University. His research interests include wireless sensor network, energy efficiency, security, and WSN health applications.



network protocol design, resource allocation and optimisation, network-level coding, network security.

Xiaomin Chen joined the Department of Computer and Information Sciences as a Lecturer in Jan 2016. Prior to this she worked as a Research Associate in the Department of Computer Science, Loughborough University, UK from Sep 2014 to Aug 2015. From Dec 2012 to Aug 2013, she worked as a Postdoc Research Fellow in the Hamilton Institute, National University of Ireland Maynooth, where she was awarded the PhD degree in Mathematics and Wireless Networking in Sep 2013. Her research is mainly focused on wireless networking, including



Mohsin Raza is a senior lecturer at Department of Computer Science, Edge Hill University, UK. He completed his PhD at Math, Physics and Electrical Engineering Department, Northumbria University (NU), UK and BS (Hons) and MS degrees in Electronic Engineering from Mohammad Ali Jinnah University (MAJU), Pakistan. Prior to his work at Edge Hill University, he worked as a Lecturer (2019-20) at Northumbria University, UK, as a post-doctoral fellow (2018-19) at Middlesex University, UK, as a Demonstrator and Doctoral Fellow (2015-17) at Northumbria University UK, Junior lecturer (2010-12) and later as Lecturer (2012-15) in Engineering department at Mohammad Ali Jinnah University, Pakistan, and Hardware Support Engineer (2009-10) at Unified Secure Services, Pakistan. He served as a technical committee member for ICET 2012, SKIMA 2015, SKIMA 2017, WSGT 2017, CSNDSP 2018, SKIMA 2018, ICT 2019 and CSoNet 2019. He has also been a guest editor and reviewer in several special issues and journals. His research interests include IoT, 5G and wireless networks, autonomous transportation systems, machine learning, Industry 4.0 and digital twins.



Rafay Iqbal Ansari received his Ph.D. in computer engineering from the Department of Computer Science and Engineering, Frederick University, Cyprus. Currently, he is working as a Lecturer at the Department of Computer and Information Science, Northumbria University, UK. His research interests lie in optimal resource allocation, 5G device-to-device (D2D) networks, intelligent surfaces, millimeterWave networks and public safety networks.